

Hans Ulrich Schmelz · Michael Abend · Matthias Port
Michael Schwerer · Ekkehard W. Hauck
Wolfgang Weidner · Christoph Sparwasser

Comparative analysis of different apoptosis detection methods in human testicular cancer

Received: 16 September 2003 / Accepted: 8 March 2004 / Published online: 29 April 2004
© Springer-Verlag 2004

Abstract In situ end-labeling (ISEL) of internucleosomal 3' DNA strand breaks and the morphological proof of nuclear chromatin condensation are two widely used methods to investigate and quantify apoptosis. However, it is still unclear whether both processes are linked with each other and if quantifying apoptosis by both methods leads to comparable results. Therefore, internucleosomal DNA fragmentation and chromatin condensation were measured simultaneously on double-fluorescence-labeled sections of 62 testicular tumors (47 nonseminomatous tumors and 15 seminomas) using immunofluorescence microscopy. Different apoptotic indices (AI), based on DNA fragmentation and/or morphological criteria were determined. The AI were quantified. Morphologically obtained AI ranged between 1.99% for non-seminomatous tumors and 0.88% for seminomas. The detection of DNA fragmentation values ranged between 8.15% for non-seminomatous tumors and 2.70% for seminomas. Only about 30% of all apoptotic cells could be detected with the morphological method compared to 80% using ISEL in both tumor entities. Therefore, the equivalence of investigations using different apoptosis detection methods in human testicular cancer seems questionable.

Keywords Apoptosis · Testicular cancer · DNA fragmentation · Chromatin condensation · Detection method

Introduction

Apoptosis is known as a multistep process characterized by internucleosomal DNA cleavage and condensation of the chromatin leading to a non-homogenous chromatin distribution along the nuclear membrane. The method of choice for the detection of internucleosomal DNA cleavage is the in situ end-labeling (ISEL) of 3'-DNA strand breaks using a fluorescent dye [1, 2]. Morphological changes, such as chromatin condensation, can be visualized with a DNA-specific fluorescent dye [3].

Apoptosis induction plays a crucial role in the therapy of testicular cancer patients. It is one of the major effects of chemotherapeutic drugs and is essential to the good prognosis of testicular cancer patients. On the other hand, chemotherapy resistance, with a poor prognosis for the patients, can be a consequence of altered apoptotic programmes [4, 5]. Consequently the efficacy of cytotoxic drugs is assessed by quantifying apoptosis [6]. It is therefore vital to have reliable methods for the detection and also for the quantification of cell death [7].

So far, however, it is unclear whether the morphologically characterized condensation of chromatin as well as biochemically investigated DNA fragmentation are linked with each other [8]. Preliminary investigations performed on testicular cancer showed a three to four-fold higher rate of apoptotic cells detected with ISEL compared to the morphological method [9]. Therefore, it is unclear whether quantifying apoptosis with either method will lead to comparable results. The comparability of investigations using different apoptosis detection methods seems questionable. Nevertheless, either the morphological or the biochemical detection method are used exclusively in in vivo studies in order to determine the proportion of apoptotic cells in tissue [10, 11, 12, 13].

H. U. Schmelz (✉) · C. Sparwasser
Department of Urology, Federal Armed Forces Hospital,
Oberer Eselsberg 40, 89081 Ulm, Germany
E-mail: Hans.U.Schmelz@web.de
Tel.: +49-731-17102101
Fax: +49-731-17102108

M. Abend · M. Port
Institute of Radiobiology, Federal Armed Forces
Medical Academy, Munich, Germany

M. Schwerer
Department of Pathology, Federal Armed Forces Hospital,
Ulm, Germany

H. U. Schmelz · E. W. Hauck · W. Weidner
Department of Urology, Justus Liebig University,
Giessen, Germany

The aim of this study was to quantify apoptosis using both methods in order to define the apoptotic detection method most suitable for routine apoptosis quantification. These examinations were performed for the first time in a large in vivo series on 62 testicular tumors.

Materials and methods

Tissue

Tissue samples obtained from 62 patients with testicular cancer (47 non-seminomatous germ cell tumors NSGCT: 26 pure embryonal cell carcinomas and 21 mixed germ cell tumors; as well as 15 seminomas) were examined. The cases were selected from the files of diagnosed surgical specimens at the Department of Pathology, Military Hospital, Ulm, Germany. Paraffin embedded tissues were fixed in 4% buffered formalin and processed by standard methods. Two consecutive 5 μ m cut sections were mounted per coated slide (Superfrost/Plus, Menzel Gläser, Munich, Germany). One section was processed for ISEL of DNA fragments employing the Apop Tag plus Apoptosis Detection Kit (Oncor, Appligene, Heidelberg, Germany). The remaining section was stained with hematoxylin and eosin to define the tumor region under the guidance of an experienced pathologist.

Microdissection was not performed in NSGCT because the number of cases of each subtype which could be evaluated was too small to find significant differences between the histological components (embryonal cell carcinoma $n=17$, yolk sac carcinoma $n=6$, chorion carcinoma $n=5$, seminoma $n=5$, mature teratoma $n=3$, immature teratoma $n=6$). The number of cases which could be evaluated was even less, because in some of the tumors the proportion of the relevant region was too small to investigate with enough microscopic fields for a representative cell count for the specific tumor entity to be made.

To get an impression of whether there might be possible differences between histological subtypes, however, pure embryonal cell carcinomas were investigated separately.

All investigations were performed after approval by the local Human Investigations Committee.

In situ end-labeling and DNA counterstaining

The ApopTag Plus Kit (Oncor, Appligene, Heidelberg, Germany) was used for ISEL, as recently published [9]. In brief, after deparaffination, tissue sections were incubated with 20 μ g/ml proteinase K (Boehringer Mannheim) diluted in distilled water for 8 min at 37°C, washed in distilled water (four times), incubated with TdT mix according to the manufacturer's protocol for 60 min at 37°C in a humidified chamber, washed three times in distilled water and incubated with anti-dig-FITC for 30 min at room temperature in a humidified

chamber. The DNA dye, 4',6-diamino-2-phenylindole (DAPI, final concentration 1.0 μ g/ml; Serva, Heidelberg, Germany) was added for examination of the nuclear apoptosis morphology and incubated for 5 min. Slides were washed three times with distilled water, dried at room temperature and either mounted in glycerol/paraphenylenediamine (PPD, antifading drug; final concentration 1 mM, Aldrich, Steinheim, Germany) or stored at 4° C and mounted immediately before examination. HL-60 cells (which served as a positive control) were treated similarly, except for omitting the first treatment step with proteinase K. For negative controls, TdT was not added to the reaction mixtures. The optimization of the method (e.g. duration of proteinase K exposure) was determined in a cascade of preliminary experiments (not shown). Cells with a FITC signal in the nucleus were considered to contain fragmented DNA.

After nuclear staining using DAPI as a DNA specific dye, cells were differentiated into: (1) morphologically non-apoptotic cells, characterized by a homogeneous distribution of DNA in the normal sized nucleus, and (2) morphologically apoptotic cells showing a condensed DNA along the nuclear membrane.

The proportion of apoptotic cells was quantified by calculating the apoptotic index (AI), i.e. the percentage of apoptotic cells in all investigated cells of the tumor.

Microscopic examination and definition of apoptotic indices

The slides were scored for the two types of cells (magnification: 400 \times) with the aid of an epifluorescence microscope (Orthoplan; Leica, Wetzlar, Germany) equipped with a filter block for DAPI excitation (excitation: 270–380 nm; emission: 410–580 nm). When changing the filter block with the filter wheel, the same cells were examined for FITC signals (excitation: 450–490 nm; emission: ≥ 520 nm, long pass filter) enabling us to differentiate between morphologically normal cells and morphologically apoptotic cells which either bore FITC signals (DNA fragmentation) or not.

This led to three AI: (1) AI of morphologically normal cells showing DNA fragmentation ($AI_{DNA\text{ frag}}$), (2) AI of morphologically apoptotic cells with DNA fragmentation ($AI_{frag+cond}$), and (3) AI of morphologically apoptotic cells without DNA fragmentation ($AI_{chrom\ cond}$) (Table 1).

The sum of these AIs was considered to represent all apoptotic cells that could be detected in the tissue section ($AI_{all\ apopt}$).

However it may not be convenient for the routine quantification of apoptosis to check every single cell for both morphological and biochemical (ISEL) features. It would be much easier to use only one detection method. The question arose as to whether the quantification of apoptosis with either ISEL or apoptotic morphology would lead to results comparable to those of the above described "single cell method".

Table 1 Cellular apoptotic features in different apoptotic indices (AI)

AI	DNA fragmentation (ISEL)	Apoptotic morphology
AI _{frag}	+	–
AI _{chrom cond}	–	+
AI _{frag+cond}	+	+
AI _{morphology}	±	+
AI _{ISEL}	+	±

Therefore, two additional AIs, obtained by performing one detection method without considering the second, were calculated (Table 1): (1) the percentage of all cells showing apoptotic nuclear morphology on DAPI staining (AI_{chrom cond} + AI_{frag+cond}) This AI was named AI_{morphology}, (2) the percentage of all cells showing DNA fragmentation after ISEL (AI_{frag} + AI_{frag+cond}). This was named AI_{ISEL}.

It is evident that quantifying apoptosis with only one method ignores a certain amount of apoptotic cells. On the other hand, it is not clear to what extent the addition of both would overestimate the apoptotic index of a tissue section. Therefore, the sum of AI_{morphology} and AI_{ISEL} was calculated (= AI_{ISEL+morphology}).

The mathematically obtained AIs, AI_{morphology}, AI_{ISEL} and AI_{ISEL+morphology} were compared with the AIs obtained by microscopic evaluation on a single cell basis.

Statistics

The mean and SD as well as significance levels (*t*-test or Mann-Whitney Rank Sum Test if the equal variance test failed) were calculated with the aid of statistical software (Sigma Stat for Windows, 2.0; Jandel, Erkrath, Germany).

Results

DNA fragmentation and chromatin condensation in apoptotic testis tumor cells

On a single cell basis, the proportion of cells showing only DNA fragmentation (AI_{DNA frag}), only chromatin

condensation (AI_{chrom cond}) or DNA fragmentation and chromatin condensation (AI_{frag+cond}) were assessed.

In all NSGCT investigated, AI_{DNA frag} (7.37% ± 10.4) was significantly higher than AI_{chrom cond} (1.20% ± 1.74) and AI_{frag+cond} (0.78% ± 1.0) (*P* < 0.001) (Fig. 1). A similar distribution could be found for seminomas (AI_{DNA frag} (2.30% ± 1.7), AI_{chrom cond} (0.49% ± 0.4), AI_{frag+cond} (0.39% ± 0.3) (*P* < 0.001).

The proportion of cells that can be recognized with one detection method

With ISEL, three to fourfold more apoptotic cells could be detected compared to the morphological method. For NSGCT, AI_{ISEL} was 8.15% ± 10.2 compared to AI_{morphology} 1.99% ± 2.4 (*P* < 0.001). A similar difference could be found in seminomatous tumors (AI_{ISEL} 2.70% ± 1.8 vs AI_{morphology} 0.88% ± 0.56).

Consequently, there was a significant difference in the proportion of apoptotic cells that can be detected by performing ISEL or nuclear staining. For NSGCT, 83.60% ± 17.72 of all apoptotic could be found with ISEL compared to 28.74% ± 26.51 with the morphological nuclear staining (*P* < 0.001). In seminomas, similar results were found with 83.45% ± 10.45 of all apoptotic cells being detected with ISEL compared to 33.67% ± 19.33 with the morphological method (*P* < 0.001, *t*-test) (Fig. 2).

There was no difference between pure embryonal cell carcinoma and mixed NSGCT.

Difference between AI_{all apop} and AI_{ISEL+Morphol}

In NSGCT there was no significant difference between AI_{ISEL+morphology} (10.14 ± 10.5) and AI_{all apop} (7.99 ± 6.8). The same was found in seminoma (AI_{ISEL+morphology} (3.58 ± 2.2) and AI_{all apop} (3.18 ± 2.0) (Fig. 3).

Quantification of the apoptotic indices

For morphologically defined apoptosis detection, we identified apoptotic indices between 1.99% for non-

Fig. 1 A comparison of AI_{DNA frag}, AI_{chrom cond} and AI_{frag+cond} in NSGCT and seminomas. AI_{DNA frag} was significantly higher than AI_{chrom cond} or AI_{frag+cond} in both entities

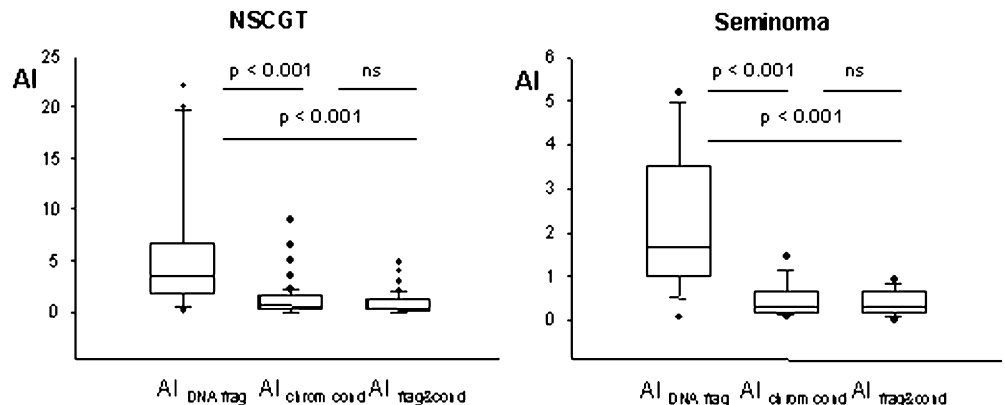


Fig. 2 The difference in the percentage of apoptotic cells that can be recognized with one of both detection methods. In NSGCT and seminomas, a three to fourfold higher percent of apoptotic cells is recognized with in situ end-labeling

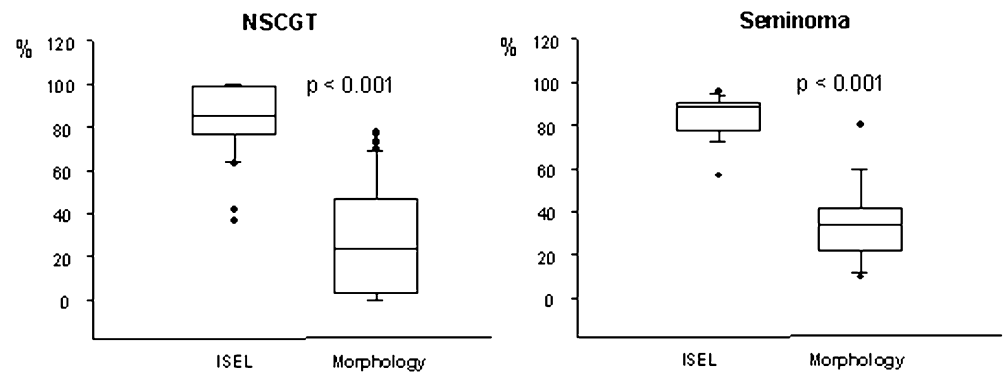


Fig. 3 The difference between $AI_{(ISEL + morphology)}$ representing the AI obtained by adding AI_{ISEL} and $AI_{morphology}$, and $AI_{all\ apop}$ representing all apoptotic cells

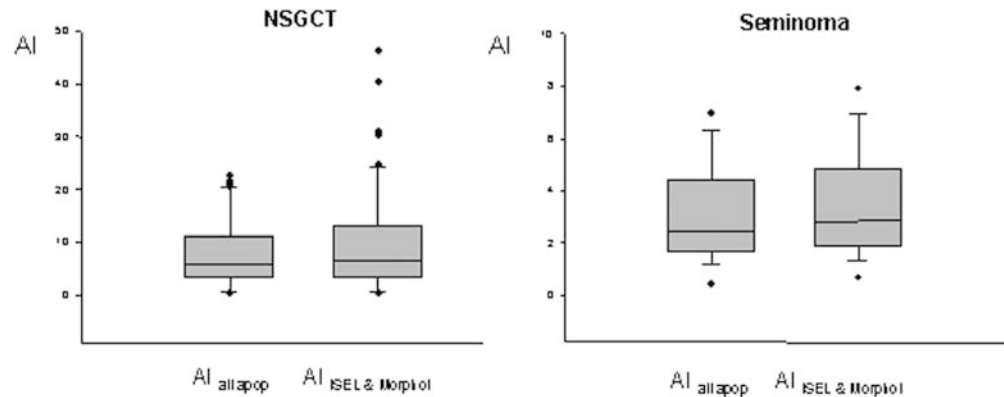


Table 2 Quantification of apoptosis. AI for all investigated subgroups (mean \pm standard deviation) (NSGCT = non-seminomatous germ cell tumors)

	$AI_{DNA\ frag}$	$AI_{chrom\ cond}$	$AI_{frag + cond}$	AI_{ISEL}	$AI_{morphology}$
All NSGCT	$n = 47$ 7.37 ± 10.38	$n = 47$ 1.20 ± 1.74	$n = 47$ 0.78 ± 1.01	$n = 47$ 8.15 ± 10.26	$n = 47$ 1.99 ± 2.49
All mixed NSGCT	$n = 21$ 6.11 ± 6.40	$n = 21$ 1.34 ± 1.53	$n = 21$ 0.49 ± 0.61	$n = 21$ 7.59 ± 8.78	$n = 21$ 1.84 ± 1.97
All pure embryonal cell carcinomas	$n = 26$ 5.92 ± 6.85	$n = 26$ 1.09 ± 1.92	$n = 26$ 1.02 ± 1.33	$n = 26$ 8.61 ± 11.48	$n = 26$ 2.11 ± 2.87
All metastasised NSGCT	$n = 23$ 7.50 ± 10.85	$n = 23$ 1.01 ± 1.40	$n = 23$ 0.99 ± 1.30	$n = 23$ 8.49 ± 10.69	$n = 23$ 2.01 ± 2.27
All non-metastasised NSGCT	$n = 24$ 7.25 ± 9.98	$n = 24$ 1.38 ± 2.03	$n = 24$ 0.59 ± 0.84	$n = 24$ 7.83 ± 10.06	$n = 24$ 1.97 ± 2.73
All seminomas	$n = 15$ 2.3 ± 1.68	$n = 15$ 0.49 ± 0.40	$n = 15$ 0.39 ± 0.29	$n = 15$ 2.70 ± 1.78	$n = 15$ 0.88 ± 0.56
All metastasised seminomas	$n = 5$ 1.4 ± 1.16	$n = 5$ 0.34 ± 0.46	$n = 5$ 0.32 ± 0.27	$n = 5$ 1.72 ± 1.15	$n = 5$ 0.66 ± 0.56
All non-metastasised seminomas	$n = 10$ 2.75 ± 1.77	$n = 10$ 0.56 ± 0.38	$n = 10$ 0.43 ± 0.32	$n = 10$ 3.18 ± 1.87	$n = 10$ 0.99 ± 0.56

seminomatous tumors and 0.88% for seminomas. With ISEL, i.e. the detection of DNA fragmentation, significantly higher rates of apoptotic cells could be detected. These values ranged between 8.15% for non-seminomatous tumors and 2.70% for seminomas (Table 2).

Discussion

Apoptosis and its regulation play an important role in the pathogenesis and therapy of human testicular cancer, being the major effect of chemotherapeutic drugs

[4, 5]. Chemoresistance is linked with altered apoptotic programmes [5]. A great deal of research is therefore aimed at defining the molecular mechanisms that play a role in apoptosis in testicular tumors [14, 15, 16, 17, 18, 19]. As one of the common end points of experiments related to apoptosis is the death of the cell, it is vital to have reliable and reproducible methods for the detection of, and especially for the quantification of, cell death [7, 23].

The definition of apoptosis is mainly based on two hallmarks of the process, i.e. DNA fragmentation [24] and the typical apoptotic morphology of the cells [3].

Both features can also be used for identifying apoptotic cells using ISEL for the detection of DNA fragmentation [1, 2] and nuclear staining with a DNA specific dye (DAPI) for the assessment of morphological changes [3].

Most of the recent studies dealing with apoptosis in human testicular cancer, however, have used only one of these methods [10, 12, 14, 16], although it was hypothesized that both processes are not linked with each other in this tumor entity [9].

Therefore, the question arises of whether AI, obtained by *in situ* end-labeling or by the investigation of apoptosis morphology, will give comparable results. The present investigation was performed to quantify the amount of apoptosis *in vivo* in testicular cancer using both methods and to define the detection method most suitable for routine apoptosis quantification.

For the first time, it could be shown that there is a significant difference between the apoptotic index obtained by ISEL and by the investigation of apoptotic morphology in human testicular cancer (NSGCT and seminomas). In NSGCT, as well as in seminomas, AI_{ISEL} was about threefold higher than $AI_{morphology}$. Only 25–30% of all apoptotic cells could be detected with the morphological approach. With ISEL, the proportion increased to 80%, but still 15–20% of all apoptotic cells were missed.

The reason for this huge difference can be found by considering both apoptotic features on a single cell basis. DNA fragmentation was found in 70% of all apoptotic tumor cells, but only 16% had an apoptotic morphology. This means that 86% of all apoptotic tumor cells express only one of both apoptotic features, leading to a significant failure in the AI determined using only one detection method.

Consequently, the most accurate way to determine the AI of human testicular tumors would be to investigate DNA fragmentation and apoptotic morphology for every single cell and to add $AI_{DNA\ frag}$, $AI_{chrom\ cond}$ and $AI_{frag\ and\ cond}$, thus obtaining the proportion of all apoptotic cells in a tissue section. In the present investigation, we called this $AI_{all\ apop}$. However, as described above, this method is very time consuming and seems at least impractical, even if performed with the aid of an image analyzing system. Therefore it seems reasonable to look for a more practical way to determine an accurate AI for tissue.

Only a small proportion of all apoptotic cells show both apoptotic features simultaneously. Therefore, adding AI_{ISEL} and $AI_{morphology}$ could lead to comparable results to the addition of all apoptotic indices obtained at a single cell level. Indeed, there was no difference between $AI_{ISEL} + AI_{morphology}$ and $AI_{all\ apop}$. At least for testicular cancer, this might be an appropriate way to quantify apoptosis. It avoids the time consuming investigation of DNA fragmentation and apoptotic nuclear morphology for every cell in a tissue section.

Several groups have compared different detection methods in certain cell systems or tissues with incon-

sistent results. A close correlation could be found between apoptosis morphology and ISEL in embryonal tissue [25] and in different paraffin embedded normal and tumor tissues [26]. Others could not identify any correlation [7], or they found it to be cell system dependent [27].

One reason why most of the cells show one apoptotic feature only may be an independent activation of two genetic programs for DNA fragmentation and chromatin condensation. Several studies support the hypothesis of such an independent activation in testicular cancer. Evidence for this was based especially on the finding that most of the apoptotic bodies representing the final stage of the apoptotic process revealed no DNA fragmentation. At least in this stage the occurrence of both apoptotic features should be expected [9, 28]. In other systems, morphological features of apoptosis occur in the absence of DNA fragmentation [29, 30]. Finally enucleated cells incubated with the apoptosis inducing antibody APO-1/Fas revealed the key morphological features of apoptosis. In non-enucleated cells, inhibitors of endonucleases blocked DNA fragmentation but not cell death induced by anti-APO-1. These data provide further evidence for an independent activation of DNA fragmentation and chromatin condensation [31].

Little information on the mechanisms of the independent activation of DNA fragmentation and chromatin condensation is available for testicular cancers. Additional investigations are therefore required to address the field of regulation of apoptotic cell death in this tumor.

Our results show clearly that the detection method used for calculating AI must be specified, because there are significant differences in the proportion of apoptotic cells using different apoptosis detection methods.

There are few studies that assess AI in human testicular cancer by ISEL [8, 13]. All investigations found AI_{ISEL} to be within about the same range as we did. The other AI have not been assessed so far in testicular cancer *in vivo*.

Conclusion

This study showed a three to fourfold higher detection rate of apoptosis using the ISEL technique compared to the morphological method in human seminoma and NSGCT. Therefore, the interpretation and comparison of studies dealing with apoptosis must be carried out with caution, especially if different apoptosis detection methods were used.

A combined approach, using both morphological and biochemical detection methods, should allow the quantification of the amount of apoptotic cell death in testicular cancer and other tumors more precisely. Comparable and reliable methods for the investigation of apoptosis are prerequisites for the investigation of this event as the major biological phenomenon in the therapy of testicular cancer.

Acknowledgement The authors would like to thank the German Department of Defense, which supported this study generously (51K 3 S 14 99 00).

References

1. Davison FD, Groves M, Scaravilli F (1995) The effects of formalin fixation on the detection of apoptosis in human brain by in situ end-labeling of DNA. *Histochem J* 27: 983
2. Isaac JT (1994) Advances and controversies in the study of programmed cell death/apoptosis in the development of and therapy for cancer. *Curr Opin Oncol* 6: 82
3. Kerr JFR, Wyllie AH, Currie AR (1972) Apoptosis: a basic biological phenomenon with wide ranging implications in tissue kinetics. *Br J Cancer* 26: 1790
4. Spierings DC, DeVries EG, Vellenga E, De Jong S (2003) The attractive Achilles heel of germ cell tumors: an inherent sensitivity to apoptosis inducing stimuli. *J Pathol* 200: 137
5. Mayer F, Stoop H, Scheffer GL, Scheper R, Oosterhuis JW, Looijenga LH, Bokemeyer C (2003) Molecular determinants of treatment response in human germ cell tumors. *Clin Cancer Res* 9: 767
6. Dunkern TR, Mueller-Klieser W (1999) Quantification of apoptosis induction by doxorubicin in three types of human mammary carcinoma spheroids. *Anticancer Res* 19: 3141
7. Leite M, Quinta-Costa M, Leite PS, Guimaraes JE (1999) Critical evaluation of techniques to detect and measure cell death—study in a model of UV radiation of the leukaemic cell line HL 60. *Anal Cell Pathol* 19: 139
8. Robertson JD, Orrenius S, Zhivotovsky B (2000) Nuclear events in apoptosis. *J Struct Biol* 129: 346
9. Abend M, Schmelz HU, Kraft K, Rhein AP, Van Beuningen D, Sparwasser C (1998) Intercomparison of apoptosis morphology with DNA cleavage on single cells in vitro and on testis tumors. *J Pathol* 185: 419
10. Soini Y, Pääkkö P (1996) Extent of apoptosis in relation to p53 and bcl-2 expression in germ cell tumors. *Human Pathol* 27: 1221
11. Meachem SJ, McLachlan RI, Stanton PG, Robertson DM, Wreford NG (1999) FSH immunoneutralization acutely impairs spermatogonial development in normal adult rats. *J Androl* 20: 756
12. Ikeda M, Kodama H, Fukuda J, Shimizu Y, Murata M, Kumagai J, Tanaka T (1999) Role of radical oxygen species in rat testicular germ cell apoptosis induced by heat stress. *Biol Reprod* 61: 393
13. Young KA, Zirkin BR, Nelson RJ (1999) Short photoperiods evoke testicular apoptosis in white-footed mice (*Peromyscus leucopus*). *Endocrinology* 140: 3133
14. Yakirevich E, Lefel O, Sova Y, Stein A, Cohen O, Izhak OB, Resnick MB (2002) Activated status of tumour-infiltrating lymphocytes and apoptosis in testicular seminoma. *J Pathol* 196: 67
15. Behrens P, Jeske W, Wernert N, Wellmann A. (2001) Down-regulation of clusterin expression in testicular germ cell tumours. *Pathobiology* 69: 19
16. Grobholz R, Verbeke CS, Schleger C, Kohrmann KU, Hein B, Wolf G, Bleyl U, Spagnoli GC, Coplan K, Kolb D, Iversen K, Jungbluth AA (2000) Expression of MAGE antigens and analysis of the inflammatory T-cell infiltrate in human seminoma. *Urol Res* 28: 398
17. Schmelz HU, Abend M, Kraft K, Hauck EW, Weidner W, Van Beuningen D, Sparwasser C (2002) Fas/Fas ligand system and apoptosis induction in testicular carcinoma. *Cancer* 95: 73
18. Burger H, Nooter K, Boersma AW, Van Wingerden KE, Looijenga LH, Jochemsen AG, Stoter G. (1999) Distinct p53-independent apoptotic cell death signalling pathways in testicular germ cell tumour cell lines. *Int J Cancer* 81: 620
19. Roelofs H, Mostert MC, Pompe K, Zafarana G, Van Oorschot M, Van Gurp RJ, Gillis AJ, Stoop H, Beverloo B, Oosterhuis JW, Bokemeyer C, Looijenga LH (2000) Restricted 12p amplification and RAS mutation in human germ cell tumors of the adult testis. *Am J Pathol* 157: 1155
20. Bala S, Oliver H, Renault B, Montgomery K, Dutta S, Rao P, Houldsworth J, Kucherlapati R, Wang X, Chaganti RS, Murty VV (2000) Genetic analysis of the APAF1 gene in male germ cell tumors. *Genes Chromosomes Cancer* 28: 258
21. Arriola EL, Rodriguez-Lopez AM, Hickman JA, Chresta CM (1999) Bcl-2 overexpression results in reciprocal downregulation of Bcl-X(L) and sensitizes human testicular germ cell tumours to chemotherapy-induced apoptosis. *Oncogene* 18: 1457
22. Heidenreich A, Schenkman NS, Sesterhenn IA, Mostofi KF, Moul JW, Srivastava S, Engelmann UH (1998) Immunohistochemical and mutational analysis of the p53 tumour suppressor gene and the bcl-2 oncogene in primary testicular germ cell tumours. *APMIS* 106: 90
23. Loo DT, Rillema JR (1998) Measurement of cell death. *Methods Cell Biol* 57: 251
24. Wyllie AH (1980) Glucocorticoid-induced thymocyte apoptosis is associated with endogenous endonuclease activation. *Nature* 284: 555
25. Ambroso JL, Stedman DB, Elswick BA, Welsch F (1998) Characterization of cell death induced by 2-methoxyethanol in CD-1 mouse embryos on gestation day 8. *Teratology* 58: 231
26. Wijsman JH, Jonker RR, Keijzer R, DeVelde CJH, Cornelisse CJ, Van Dierendonck JH (1993) A new method to detect apoptosis in paraffin sections: in situ end-labeling of fragmented DNA. *J Histochem Cytochem* 41: 7
27. McCloskey TW, Chavan S, Lakshmi Tamma SM, Pahwa S (1998) Comparison of seven quantitative assays to assess lymphocyte cell death during HIV infection: measurement of induced apoptosis in anti-Fas-treated Jurkat cells and spontaneous apoptosis in peripheral blood mononuclear cells from children infected with HIV. *AIDS Res Hum Retroviruses* 14: 1413
28. Schmelz HU, Abend M, Kraft K, Van Beuningen D, Pust R, Sparwasser C (1999) Apoptosis in human embryonal cell carcinoma: preliminary results. *Urol Res* 27: 368
29. Cohen GM, Sun XM, Snowden RT, Dinsdale D, Skilleter DN. (1992) Key morphological features of apoptosis may occur in the absence of internucleosomal DNA fragmentation. *Biochem J* 286: 331
30. Falcieri E, Martelli AM, Bareggi R, Cataldi A, Cocco L (1993) The protein kinase inhibitor staurosporine induces morphological changes typical of apoptosis in MOLT-4 cells without concomitant DNA fragmentation. *Biochem Biophys Res Commun* 193: 19
31. Schulze-Osthoff K, Walczak H, Droge W, Krammer PH (1994) Cell nucleus and DNA fragmentation are not required for apoptosis. *J Cell Biol* 127: 15